

Deformation density components analysis of fullerene-based anti-HIV drugs

Sara Fakhraee · Maryam Souri

Received: 27 January 2014 / Accepted: 6 October 2014 / Published online: 13 November 2014
© Springer-Verlag Berlin Heidelberg 2014

Abstract Deformation density analysis is performed on fullerene-based anti-HIV agents to investigate the influence of charge redistribution on the capability of binding to HIV enzymes. Two types of HIV inhibitors including malonic acid- and amino acid-type C_{60} derivatives are considered to study. Total deformation density and its components including orbital relaxation and kinetic energy pressure are obtained for C_{60} derivatives. The deformation natural orbitals for each component of deformation density are assessed and their amounts of charge displacement are quantified to evaluate the binding affinity of HIV inhibitors. The results show that the orbital relaxation plays a more prominent role in deformation of electron density of studied compounds. Among the considered drugs, the amino acid-type derivatives, N-(carboxymethyl)-2,5-dicarboxylic fulleropyrrolidines, show the most charge displacement. Moreover, the investigation into the deformation density of amino acid-type functional groups on C_{60} reveals that the connection of functional groups to the 5,6-ring junction results more displaced charge than the connection to the 6,6-ring junction.

Keywords Deformation density · Deformation natural orbital · Density functional calculation · Fullerene-based anti-HIV drug · HIV inhibitor · Kinetic energy pressure · Orbital relaxation

Introduction

Special characteristics of fullerenes and their derivatives make them very applicable in medical chemistry. For example, C_{60}

can be used in gene delivery, magnetic resonance imaging agents, and drug delivery [1, 2]. Inhibition activity of fullerenes derivatives against enzymes such as glutathione transferase, glutathione reductase, and nitric oxide synthase have been widely reported [3–6]. Nevertheless, the applications of fullerenes in biological environments are limited because of their very low solubility in polar solvents [7, 8]. Thirty double bonds in C_{60} structure make it possible to add particular designed chemical functional groups to C_{60} . The addition of functional groups increases the polarity of C_{60} derivatives and makes them more soluble in polar solvents [9].

The C_{60} derivatives are suggested as greatest medical potential for human immunodeficiency virus (HIV) inhibitors [10, 11]. HIV-protease (HIV-PR) and HIV-reverse transcriptase (HIV-RT) enzymes are two targets for anti-HIV fullerene derivatives. The most offered mechanism for this inhibiting process is occupation of HIV enzyme cavity by C_{60} core [2, 12–15]. Molecular modeling studies have demonstrated that C_{60} could properly fit within the active sites of the HIV-PR core to prevent the vital activity of this enzyme [11, 13]. The activity of HIV-RT enzyme is inhibited in a similar way by fullerene-based derivatives [12]. In 2005, Mashino et al. [16] synthesized some malonic acid- and amino acid-type C_{60} derivatives and investigated the inhibitory activity of these compounds on HIV-RT. This was the first report concerning the effect of C_{60} derivatives on HIV-RT. The investigation of biological properties of HIV-RT inhibitors is a broad but immature area of research yet. On the other hand, the physical and chemical properties of C_{60} derivatives responsible for inhibiting HIV-RT have such a great biological importance that motivates us to study the electronic structure characterization of malonic acid- and amino acid-type C_{60} derivatives.

Deformation density, defined as electron density difference between a complex and its isolated fragments, is a powerful tool to investigate the electron reorganization during the molecular interactions or substitution of functional groups.

S. Fakhraee (✉) · M. Souri
Department of Chemistry, College of Sciences, Payame Noor University, P.O. Box 19395-3697, Tehran, Iran
e-mail: fakhraee@pnu.ac.ir

Deformation density of various systems has been studied both experimentally and theoretically [17–19]. Visualization of deformation density helps to identify the interactions in molecular complexes. It also provides significant improvements in drug design to achieve maximum effectiveness. The recently-developed approach by Weitao Yang and co-workers is noncovalent interaction (NCI) which enables simultaneous analysis and graphical visualization of a wide range of noncovalent interaction types in real space surface [20, 21]. Applying an optimal NCI index, calculated only from atomic coordinates and promolecular densities, enables the NCI method to visualize both attractive (van der Waals and hydrogen bonding) and repulsive (steric) interactions, based on properties of electron density and its derivatives [22].

Recently, an alternative procedure has been developed by our group to analyze deformation density, which decomposes deformation density into kinetic energy pressure and orbital relaxation contributions [23]. In addition, each of these terms has been defined as deformation natural orbitals and the corresponding displaced charges [24]. Analysis of deformation density and the related charge displacements in this way can properly describe the electronic phenomena responsible for inter- and intra-molecular interactions. The advantage of our deformation density analysis compared with NCI method is that, it provides orbital components of charge displacements due to kinetic energy pressure, orbital relaxation, and total deformation density, independently.

The aim of the present theoretical study is to take advantages of deformation density analysis to investigate the electronic structure of malonic acid- and amino acid-type C_{60} derivatives. We examine a number of proposed drugs by the present authors and Mashino HIV inhibitors in terms of total electron density deformation and also its orbital components to find out the nature and value of charge displacement in fullerene-based agents. We also make an effort to find the effect of deformation density on binding affinity of suggested HIV inhibitors. In order to investigate the effects of dispersion corrections on the charge displacements, we perform all calculations at different levels of density functional theory (DFT) with different basis sets.

Theoretical background

The total deformation density of a molecule due to the substitution of functional groups is decomposed into two essential contributions: kinetic energy pressure (KEP) and orbital relaxation (OR) [23]. The KEP, also known as steric repulsion effect in chemistry, is the virtual pressure imposed to orbitals to reach mutual orthogonality [25]. When an inter-molecular

or inter-fragment interaction takes place, the initial shape of orbitals is distorted to provide a proper nodal behavior. The final result is mutual orthogonality of orbitals. This phenomenon is a consequence of Pauli exclusion principle [26]. The OR is related to the rearrangement of charge distribution and variation in the Fock operator and Hartree-Fock orbitals during interaction. The consequence is variation of length and electronic energy of orbitals [27].

Recently our group introduced a method to decompose the deformation density into the KEP and OR contributions and characterize each contribution based on the orbital representation and displaced charges [23]. In this method, the first step is to form electron density matrix of complex, $P_{complex}^{\{\Phi\}}$ and a single matrix of the electron density for all fragments, $P_{fragments}^{\{\Phi\}}$, while a frozen geometry is considered for the fragments as they appear in the final complex. The matrix representation of $P_{fragments}^{\{\Phi\}}$ is defined as follow:

$$P_{fragments}^{\{\Phi\}} = \begin{bmatrix} P_{fragment\ 1} & \dots & 0 \\ \vdots & \ddots & \vdots \\ 0 & \dots & P_{fragment\ n} \end{bmatrix} \quad (1)$$

where Φ is atomic orbitals matrix, and can be defined as:

$$\Phi = [\Phi_{fragment\ 1} \Phi_{fragment\ 2} \dots \Phi_{fragment\ n}] \quad (2)$$

Three deformation density matrices P_{Δ}^{KEP} , P_{Δ}^{OR} , and P_{Δ}^{total} can be defined as:

$$P_{\Delta}^{KEP} = P_{fragments}^{(A)} - P_{fragments}^{\{\Phi\}} \quad (3)$$

$$P_{\Delta}^{OR} = P_{complex} - P_{fragments}^{(A)} \quad (4)$$

$$P_{\Delta}^{total} = P_{complex} - P_{fragments}^{\{\Phi\}} \quad (5)$$

In Eqs. 3 and 4, the superscript (A) denotes antisymmetric product of the molecular orbitals. Then deformation density responsible for KEP, OR, and total are obtained by following equations:

$$\Delta\rho_{KEP} = \Phi P_{\Delta}^{KEP} \Phi^{\dagger} \quad (6)$$

$$\Delta\rho_{OR} = \Phi P_{\Delta}^{OR} \Phi^{\dagger} \quad (7)$$

$$\Delta\rho_{total} = \Phi P_{\Delta}^{total} \Phi^{\dagger} \quad (8)$$

Each component of deformation density could be defined in terms of the space responsible for reorganization of

electrons, $\theta_{\Delta,i}$, and respective displaced charge, $n_{\Delta,i}$ as the following procedure [24]:

$$\Delta\rho = \sum_i n_{\Delta,i} |\theta_{\Delta,i}|^2 \tag{9}$$

Diagonalization of the deformation density matrix results deformation natural orbitals (DNOs), θ_{Δ} , and their corresponding eigenvalues, n_{Δ} .

$$P_{\Delta}^{\{\Phi\}} \xrightarrow{\text{diagonalization}} P_{\Delta}^{\{\Phi\}} S^{\{\Phi\}} C_{\Delta}^{\{\Phi\}} = C_{\Delta}^{\{\Phi\}} n_{\Delta} \tag{10}$$

$$\theta_{\Delta} = \Phi C_{\Delta}^{\{\Phi\}} \tag{11}$$

The n_{Δ} reflects the magnitude of displaced charge in the space defined by θ_{Δ} . $S^{\{\Phi\}}$ and $C_{\Delta}^{\{\Phi\}}$ are the overlap matrix of atomic orbitals and the eigenvectors of DNOs, respectively.

Therefore, $\Delta\rho_{KEP}$ and $\Delta\rho_{OR}$ can be defined as:

$$\Delta\rho_{KEP} = \sum_i^m n_{\Delta,i}^{KEP} |\theta_{\Delta,i}^{KEP}|^2 \tag{12}$$

$$\Delta\rho_{OR} = \sum_i^m n_{\Delta,i}^{OR} |\theta_{\Delta,i}^{OR}|^2 \tag{13}$$

where m is the number of basis elements, $\theta_{\Delta,i}^{KEP}$ and $\theta_{\Delta,i}^{OR}$ are DNOs originated from KEP and OR components, respectively, and the $n_{\Delta,i}^{KEP}$ and $n_{\Delta,i}^{OR}$ are their corresponding displaced charges. The total deformation density is decomposed as:

$$\Delta\rho_{total} = \Delta\rho_{KEP} + \Delta\rho_{OR} = \sum_i^m n_{\Delta,i}^{KEP} |\theta_{\Delta,i}^{KEP}|^2 + \sum_i^m n_{\Delta,i}^{OR} |\theta_{\Delta,i}^{OR}|^2 \tag{14}$$

Indeed, KEP is related to the exchange-repulsion in the theory of intermolecular forces [28], which arises between pairs of electrons of the same spin in interacting molecules. Intermolecular forces between two interaction molecules are also governed by electrostatic contributions. The first- and second-order electrostatic interactions arise from the classical interaction between the static charge distributions of two molecules. The second-order electrostatic contribution describes induction and dispersion effects for two interacting molecules. The dispersion has an important effect on the biological system interactions. It occurs because the charge distributions of interacting molecules are fluctuating as the electrons move. Electrons of two interacting molecules become correlated as they reach the low-energy configurations. Especially, dispersion has an important role in aggregating non-polar hydrophobic molecules in aqueous solution. Hence, dispersion contributes to the strength of the hydrophobic

interactions between C_{60} cavity and non-polar sites of enzyme.

In the original paper by the present author [23] OR component of charge displacement includes all physical interactions between the fragments, except for the Pauli repulsion. In contrast to energy decomposition, which provides electrostatic energy component between frozen fragments, our formalism includes both electrostatic and dispersion interactions in the OR component. Therefore, OR is not exactly the same as first-order electrostatics; instead, if the employed theoretical level for wave function calculation does account for dispersion interaction, it includes dispersion as well. Since hydrophobic interactions are heavily based on dispersion forces, if one wishes to inspect them via DFT methods, it must account for dispersion interactions.

It should be noted that, fragment's geometries could certainly influence how the charge density is reorganized during the complex formation. Also, the relative contribution of OR in comparison to KEP depends on the geometry used for the analysis. However, our formalism restricts us to apply frozen geometries for the fragments [23, 24].

Computational details

In this research, the deformation electron density for six fullerene-based anti-HIV drugs, represented in Fig. 1, is investigated based on the method described above.

Mashino et al. [16] investigated the anti-HIV characteristic of compounds 1, 2, and 3, experimentally. Compound 1 is a dimalonic acid derivative of C_{60} , while 2 and 3 are amino acid-type derivatives. In order to investigate a wider range of

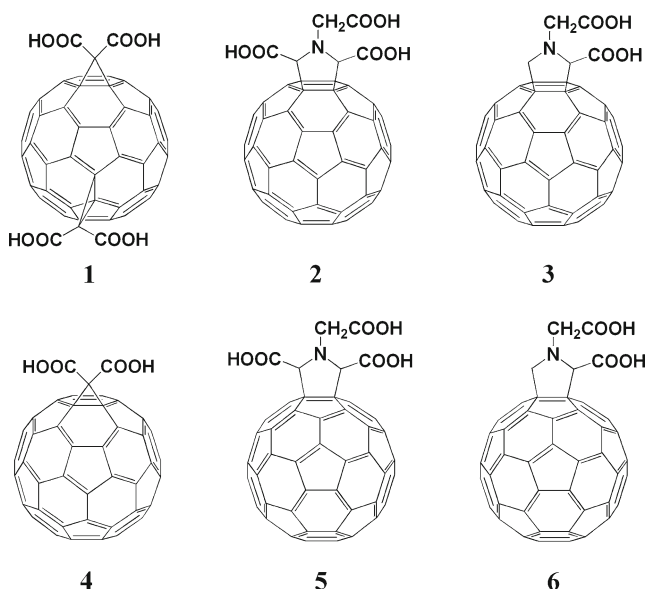


Fig. 1 Structure of two malonic acid-type (1,4) and four amino acid-type (2, 3, 5, 6) C_{60} derivatives as anti-HIV agents

C_{60} derivative drugs theoretically, we suggested three more compounds **4**, **5**, and **6** with remarkable structural similarity to Mashino drugs **1**, **2**, and **3**, correspondingly. Comparing with compound **1**, compound **4** is a mono substituted malonic acid derivative of C_{60} . Compounds **5** and **6** are amino acid-type derivatives. In compounds **5** and **2**, the functional groups are identical. The difference between these two compounds is in functional group junction. There are two types of ring junctions in C_{60} : junction of two six-membered rings (6,6-junction), and junction of five- and six-membered rings (5,6-junction). In compound **5**, the functional group is connected to the 5,6-junction, while in compound **2** the functional group is attached to the 6,6-junction. The functional groups in compounds **6** and **3** are also identical and the difference is in the location of the connectivity to C_{60} , similar to **5** and **2**, respectively.

The geometry of all compounds has been optimized in hybrid density functional B3LYP at double-zeta basis set of 6–31G(d), using Gaussian 03 suite of programs [29]. Vibrational frequencies have been calculated at the same level of theory. It has been demonstrated that all optimized structures are in local minima. Deformation density isosurfaces and deformation natural orbitals have been modeled by GaussView 5.0.8 program [30]. In order to include dispersion corrections on the deformation densities and the corresponding charge displacements, all calculations have been performed for compounds **2** and **5** using the dispersion corrected functionals B97D [31] and M06-2X [32]; the latter includes the dispersion effects directly on the electron density of system. Additionally, the effect of polarization basis functions on the calculated results has been investigated by comparing the calculated deformation densities at two different Ahlrichs basis sets, including triple-zeta valence, TZV, and triple-zeta valence polarized, TZVP [33, 34] basis sets in Gaussian 09 program [35].

The method introduced by our group in previous works [23, 24] has been used to obtain the DNOs and the respective eigenvalues. To perform deformation density analyses, electron density due to C_{60} and functional groups is obtained whereas their structure has been considered as it was in the complex.

For the sake of simplicity, the considered complexes are classified into two categories: Mashino drugs, **1–3**, and theoretical suggested drugs, **4–6**.

Results and discussion

For Mashino drugs, **1–3**, the total deformation density has been analyzed and decomposed into KEP and OR contributions. The deformation density isosurfaces corresponding to the total, KEP and OR have been calculated and represented in Table 1. The value of displaced charge for each isosurface,

$n_{\Delta,i}(i=total,KEP,OR)$, has been shown in parentheses below the surfaces. The positive value for displaced charge means concentration of electron density, while the negative value indicates depletion of electron density.

As has been shown in Table 1, the $\Delta\rho_{KEP}$ isosurfaces with negative eigenvalues are concentrated around the connecting bond between functional groups and C_{60} . It means that the KEP causes the removal of electron density from these areas. On the other hand, the $\Delta\rho_{KEP}$ isosurfaces with positive eigenvalues cover the areas of both sides of connecting bond of functional groups to C_{60} . Considering all $\Delta\rho_{KEP}$ isosurfaces with negative and positive eigenvalues at a glance, the KEP leads electron density from the middle part of the bond between functional group and C_{60} to either ends of the bond, so that, the electron density covers functional group and parts of the C_{60} .

As has been demonstrated in Table 1, $\Delta\rho_{OR}$ causes charge distribution to be spread in a greater area of molecular surface than $\Delta\rho_{KEP}$. Unlike the $\Delta\rho_{KEP}$, the $\Delta\rho_{OR}$ isosurfaces with positive and negative eigenvalues are almost isoform. In addition, the value of displaced charge due to $\Delta\rho_{OR}$ is greater than the corresponding value for $\Delta\rho_{KEP}$ in each compound. It is interesting that in all considered compounds, the $\Delta\rho_{OR}$ appears mainly in the $\Delta\rho_{total}$ and the shape of $\Delta\rho_{total}$ is completely affected by $\Delta\rho_{OR}$. Therefore, the orbital relaxation has more important contribution in formation of total deformation density, than the kinetic energy pressure, with providing the values of $n_{\Delta,OR}$ close to the $n_{\Delta,total}$.

The main mechanism of anti-HIV activity of fullerene derivatives is based on the occupation of hydrophobic vital site of HIV-RT enzyme with fullerene core and preventing its biological activity in proliferation of virus genome. Fullerenes have very low binding affinity within the enzyme. This problem is solved by addition of functional groups to isolated fullerenes [9]. The binding affinity of fullerene derivatives is referred to the ability of the functional groups to form hydrogen bonds with adjacent polar groups in the enzyme, and hydrophobic interaction of fullerene cage with nonpolar binding sites of enzyme cavity [11, 13, 36, 37]. The more deformation of electron density in HIV inhibitors results in more capability of binding to the HIV enzymes.

As can be seen in Fig. 1, two malonic acid functional groups have been attached to C_{60} in compound **1**, while in other compounds only one functional group has been attached to the C_{60} . The total displaced charge in compound **1** is 9.356 electrons. Calculating the deformation density due to each malonic acid shows that the contribution of each malonic acid in charge displacement is about 4.7 electrons. Although the results of deformation density analysis for compound **1**, suggested by Mashino [16], indicate that the highest value of displaced charge belongs to this compound, the bifunctionality of compound **1** makes it unreasonable to compare the value of displaced charges of **1** with **2–6** which have

Table 1 Total deformation density isosurface and its corresponding components: KEP and OR for compounds 1–3. The corresponding displaced charges, $n_{\Delta,i}$, (in electrons) are represented in parentheses below the isosurfaces

Drug	$\Delta\rho_{KEP}$		$\Delta\rho_{OR}$		$\Delta\rho_{total}$	
1	 (5.445)	 (-5.445)	 (8.212)	 (-8.212)	 (9.356)	 (-9.356)
2	 (3.258)	 (-3.258)	 (4.685)	 (-4.685)	 (6.006)	 (-6.006)
3	 (3.182)	 (-3.182)	 (4.416)	 (-4.416)	 (5.718)	 (-5.718)

The positive value for displaced charge means concentration of electron density, while the negative value indicates depletion of electron density

only one functional group. So, we do not choose the charge displacement for **1** as a maximum value. The investigation of deformation density for bi-functional group fullerene-based agents is the subject of new research by our group.

Deformation density analysis for Mashino drugs in Table 1 reveals that, both $\Delta\rho_{KEP}$ and $\Delta\rho_{OR}$ increase the electron density on functional group particularly on the oxygen atoms. This makes the terminal binding sites of functional groups ready for hydrogen bonding with neighbor polar groups. The outcome is to increase the binding affinity of the compounds. In all C_{60} derivatives in Table 1, $\Delta\rho_{OR}$ contribution causes more charge displacement than $\Delta\rho_{KEP}$, therefore the $\Delta\rho_{OR}$ has the major role in binding affinity of C_{60} derivatives.

As the magnitude of displaced charge increases, deformation density spread to the greater area of the compounds. This phenomenon decreases the nonpolar surface and hydrophobic nature of C_{60} derivatives. Nevertheless, the distance between polarized surface and hydrophobic interacting site of C_{60} derivatives are far enough to behave independently. The experimental evidences by Mashino have demonstrated that, compound **2** is the most effective anti-HIV drug among the introduced drugs in Table 1 [16]. This indicates that, although in this compound, the deformation density slightly reduces the

hydrophobic surface of C_{60} , either hydrogen bonding interaction, enhanced through the charge displacement via KEP and OR contributions, and hydrophobic interaction between enzyme cavity and inhibitor increase the inhibition efficiency of C_{60} derivative. Therefore, along with hydrophobic characteristic, the deformation density plays an important role in increasing binding affinity of C_{60} derivatives to enzyme.

To obtain more insight into deformation density, deformation natural orbitals (DNOs) and corresponding eigenvalues due to total, KEP and OR contribution have been represented in Table 2 for drugs 1–3. To save space, only DNOs with significant eigenvalues ($|n_{\Delta}| > 0.5$) have been displayed in this table. $n_{\Delta} > 0$ and $n_{\Delta} < 0$ refer to the concentration and depletion of electron density in the space provided by corresponding DNOs, respectively. An important point is that, all DNOs for these drugs have been formed in the areas around the binding sites of functional groups to C_{60} and surroundings. Therefore, the most significant charge displacement happens in these areas. A glance at θ_{Δ}^{KEP} DNOs in Table 2 reveals that, these orbitals have been specifically concentrated around the bond between the functional group and C_{60} . The θ_{Δ}^{KEP} 's with positive eigenvalues are extended to the ends of functional groups toward the oxygen atoms, in approving the binding affinity arguments. On the other hand, θ_{Δ}^{OR} 's are distributed to the

Table 2 KEP, OR and total DNOs (θ_{Δ}) for drugs 1–3. The respective eigenvalues are represented in parentheses below the DNOs

Drug	1				2				3			
DNO												
θ_{Δ}^{KEP}												
	(-1.499)	(1.499)	(-1.513)	(1.513)	(-0.905)	(0.905)	(-1.038)	(1.038)	(-0.929)	(0.929)	(-1.023)	(1.023)
θ_{Δ}^{OR}												
	(-1.994)	(1.994)	(-2.000)	(2.000)	(-1.140)	(1.140)	(-1.158)	(1.158)	(-1.066)	(1.066)	(-1.168)	(1.168)
θ_{Δ}^{total}												
	(-1.598)	(-1.608)	(1.998)	(2.000)	(-1.170)	(-1.271)	(1.384)	(1.425)	(-1.166)	(-1.258)	(1.354)	(1.421)

The positive eigenvalues indicate concentration of electron density on the isosurfaces displayed on the DNOs, while the negative eigenvalues indicate depletion of electron density for DNOs

greater areas of both sides of bond between the functional group and C_{60} . The θ_{Δ}^{OR} s reveal the important contribution of OR in total deformation density. For example in compound **1** the shape of the θ_{Δ}^{OR} with the highest eigenvalue (2.000) is quite similar to the shape of the θ_{Δ}^{total} with the highest eigenvalue (2.000). In other compounds the trace of θ_{Δ}^{OR} with the highest eigenvalues could be easily seen in overall shape of θ_{Δ}^{total} , too.

Table 3 shows the deformation density analysis for theoretical compounds **4–6**. Similarly, in this table the impressive role of KEP in depletion of electron density around the connecting bonds of functional group to C_{60} , and also, electron density concentration on the two terminal sites of the bond, has been demonstrated by deformation density isosurfaces. The same as the compounds **1–3**, $\Delta\rho_{OR}$ has the major contribution in deformation density of theoretical compounds **4–6**.

The difference between compounds **1** and **4** is in one additional malonic acid substitution in compound **1**. Comparing the two compounds shows that, dimalonic acid derivative of C_{60} has more significant deformation density and total displaced charge than mono substituted malonic acid. Compound **4** has the lowest eigenvalue of $\Delta\rho_{KEP}$, $\Delta\rho_{OR}$, and $\Delta\rho_{total}$ among the studied compounds.

Binding site of functional group to C_{60} is the only difference between **2** and **5**. In compound **2**, the functional group has been attached to the 6,6-junction (Fig. 1), but in **5**, it has been attached to the 5,6-junction. Compound **5** has higher values of $n_{\Delta, total}$, $n_{\Delta, OR}$, and $n_{\Delta, KEP}$ than compound **2**. Since, these two compounds have similar functional group and steric hindrance, the difference in deformation density and displaced charge for these compounds are only originated from the

binding sites of functional groups. Therefore, the position of functional groups on C_{60} can be considered as an effective factor in binding to the polar sites of adjacent molecules.

As mentioned before, there is such a difference between compounds **3** and **6**. Comparing $n_{\Delta, i}$ s for **3** and **6**, there is a little more $n_{\Delta, total}$ (about 0.259 electron) for **6**. It seems that the connection of functional group to the 5,6-junction in C_{60} leads to more charge displacement, and consequently, more binding affinity in amino acid-type derivatives of C_{60} .

In general, compound **5** has the highest value of $n_{\Delta, total}$ with respect to all the compounds. Therefore, it could be expected to have the most capability of binding to enzyme.

DNOs with significant eigenvalues for compounds **4–6** have been represented in Table 4. The location of DNOs for these compounds is similar to what happens for compounds **1–3** in Table 2. All DNOs in this table are concentrated around the binding region of functional groups to C_{60} . Therefore, the most significant charge displacement happens in this area. The θ_{Δ}^{KEP} with positive eigenvalues distribute the electron density to the functional groups. This behavior is seen more or less for θ_{Δ}^{OR} , too.

A considerable point is that, in compounds **4–6** the trace of θ_{Δ}^{OR} with the highest eigenvalue could be seen clearly, in the θ_{Δ}^{total} with maximum eigenvalues.

In summary, considering deformation density calculated for all compounds **1–6**, indicates that KEP and OR increase the binding affinity of C_{60} derivatives by strengthening the hydrogen binding of functional groups with neighbor polar groups. The OR has the dominant contribution in this phenomenon, because of having more displaced charge than KEP.

To explore the effect of dispersion corrections on the deformation densities and displaced charges, the structures **2** and

Table 3 The same as Table 1 for compounds 4–6

Drug	$\Delta\rho_{KEP}$		$\Delta\rho_{OR}$		$\Delta\rho_{total}$	
4	 (2.714)	 (-2.714)	 (4.224)	 (-4.224)	 (4.778)	 (-4.778)
5	 (3.261)	 (-3.261)	 (4.955)	 (-4.955)	 (6.242)	 (-6.242)
6	 (3.207)	 (-3.207)	 (4.699)	 (-4.699)	 (5.977)	 (-5.977)

5 with the highest charge displacement were selected for new calculations using B97D and M06-2X methods. These methods belong to the two different classes of dispersion corrected functionals in Grimme's classification [31]. The generalized-gradient approximation (GGA) type density

functional B97D has been explicitly parameterized by including damped atom-pairwise dispersion correction term of the form C_6/R^6 [31, 38, 39]. This term is not dependent on the density of the system and only affects it indirectly via geometry changes. On the other hand, the M06-2X hybrid meta-

Table 4 The same as Table 2 for compounds 4–6

Drug \ DNO	4		5				6				
θ_{Δ}^{KEP}	 (-1.514)	 (1.514)	 (-0.970)	 (0.970)	 (-1.010)	 (1.010)	 (-0.984)	 (0.984)	 (-1.004)	 (1.004)	
θ_{Δ}^{OR}	 (-2.000)	 (2.000)	 (-1.177)	 (1.177)	 (-1.230)	 (1.230)	 (-1.111)	 (1.111)	 (-1.235)	 (1.235)	
θ_{Δ}^{total}	 (-0.879)	 (-1.612)	 (2.000)	 (-1.196)	 (-1.313)	 (1.416)	 (1.466)	 (-1.195)	 (-1.301)	 (1.369)	 (1.479)

Table 5 Total deformation density isosurface and its corresponding components: KEP and OR for compound **2**, calculated using dispersion corrected methods (B97D and M06-2X), and different basis sets (TZV

and TZVP). The corresponding displaced charges, $n_{\Delta,i}$ (in electrons) are represented in parentheses below the isosurfaces

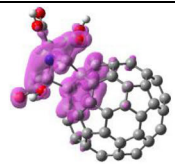
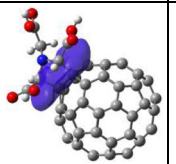
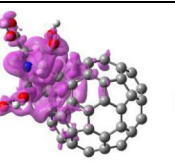
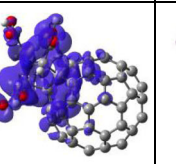
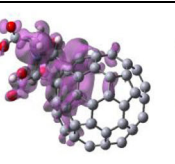
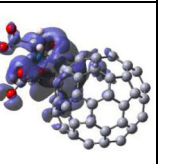
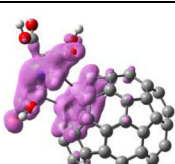
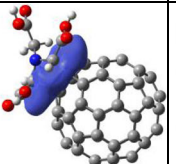
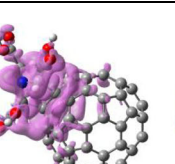
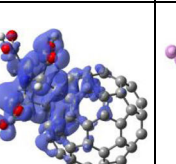
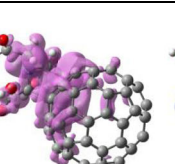
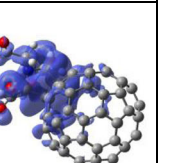
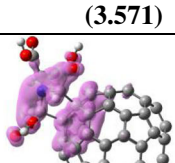
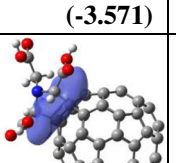
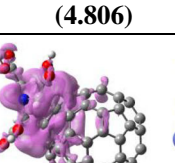
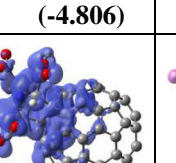
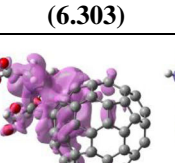
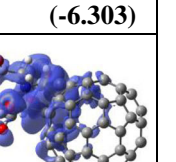
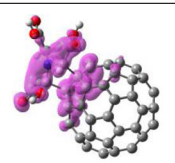
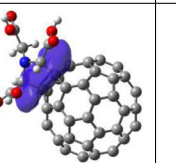
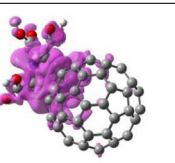
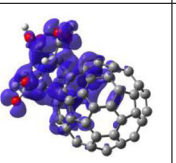
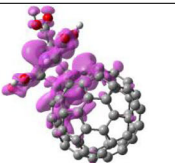
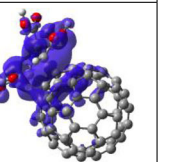
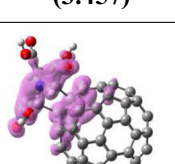
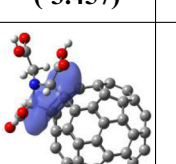
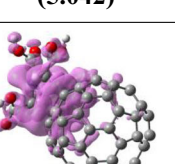
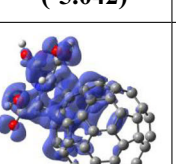
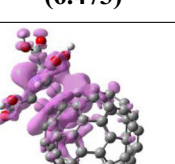
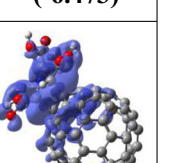
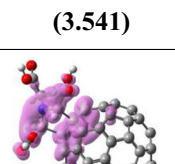
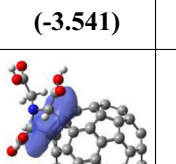
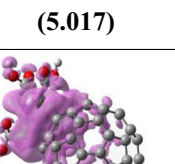
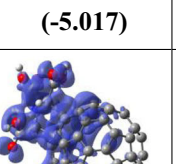
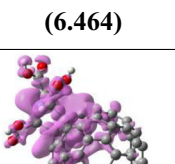
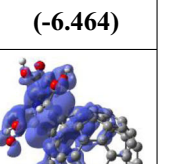
Method	$\Delta\rho_{KEP}$		$\Delta\rho_{OR}$		$\Delta\rho_{total}$	
B97D/TZV	 (3.485)	 (-3.485)	 (4.851)	 (-4.851)	 (6.330)	 (-6.330)
B97D/TZVP	 (3.571)	 (-3.571)	 (4.806)	 (-4.806)	 (6.303)	 (-6.303)
M06-2X/TZVP	 (3.593)	 (-3.593)	 (4.705)	 (-4.705)	 (6.207)	 (-6.207)

Table 6 The same as Table 5 for compound **5**

Method	$\Delta\rho_{KEP}$		$\Delta\rho_{OR}$		$\Delta\rho_{total}$	
B97D/TZV	 (3.457)	 (-3.457)	 (5.042)	 (-5.042)	 (6.473)	 (-6.473)
B97D/TZVP	 (3.541)	 (-3.541)	 (5.017)	 (-5.017)	 (6.464)	 (-6.464)
M06-2X/TZVP	 (3.576)	 (-3.576)	 (5.085)	 (-5.085)	 (6.520)	 (-6.520)

GGA functional has been heavily parameterized. This functional is purely electron density based dispersion correction and includes the dispersion contributions on electron density as well [31]. Thus, to evaluate the direct effect of dispersion corrections, calculations have also been accomplished at M06-2X functional.

Alternatively, the TZV basis set has also been selected for recent calculations. Furthermore, in order to evaluate the influence of polarization functions on deformation electron densities and displaced charges, all calculations have been repeated using the more accurate basis set, TZVP, which is augmented by polarization functions and provides one set of d-functions on heavy atoms and one set of p-functions on hydrogen atoms. Table 5 illustrates the deformation density isosurfaces and the corresponding charge displacements for compound 2, obtained via new calculations.

Comparing the value of $\Delta\rho_{KEP}$ for molecule 2, calculated at B3LYP/6-31G(d) level of theory in Table 1, with the corresponding value obtained for density functional theoretical level B97D/TZV in Table 5 shows the difference of only about 0.2 electron. Also, there is a similar difference between the values of $\Delta\rho_{OR}$ for this molecule. Deformation density isosurfaces of molecule 2, calculated by these two theoretical levels display great similarity. Comparison of calculated charge displacements obtained in B97D level for compound 2 at two different basis sets TZV and TZVP indicates the difference of about 0.1 electron for both $\Delta\rho_{KEP}$ and $\Delta\rho_{OR}$ values. Moreover, charge displacements obtained at two different B97D and M06-2X functionals with the same TZVP basis set show negligible differences. It seems that, the results provided at different theoretical levels (with and without dispersion corrections) and basis sets (with and without polarization functions) are approximately the same and the application of dispersion corrections for methods and polarization basis functions does not cause a significant variation in deformation density components and corresponding displaced charges.

Similarly, the deformation density isosurfaces and corresponding charge displacements for compound 5, obtained in different density functional levels and different basis functions, are in good agreement, too. The corresponding calculated data have been collected in Table 6.

Also, in comparing with the DNOs obtained at B3LYP/6-31G(d) level, we have found that the calculation at B97D and M06-2X theoretical levels for structures 2 and 5 results quite similar orbitals and charge displacements. Therefore, in order to save space, we have avoided inclusion of DNO figures. Therefore, in these systems, all applied theoretical levels with different basis functions provide comparable and reasonable description for explanation of deformation density components and the values of charge displacements.

Conclusions

Deformation density analysis has been performed on six C_{60} derivatives, including three experimentally examined Mashino drugs and three theoretically suggested compounds by authors. The role of components of deformation electron density, including kinetic energy pressure (KEP) and orbital relaxation (OR), to enhance polarity of C_{60} derivatives required for hydrogen bonding between functional group and polar sites of HIV-RT enzyme have been investigated theoretically. Compounds 1 and 4 are malonic acid-type and the others are amino acid-type derivatives. The deformation density resulting from functional groups in these compounds not only increases the polarity and solubility of molecule in polar environments, but also increases the binding affinity of drugs to form hydrogen bonds with neighbor polar groups.

The results show that, the OR has the main role in total deformation of electron density in studied compounds. The OR causes a widespread distribution of concentrated and depleted deformation density on some part of the C_{60} surface, functional group, and their connecting bonds. On the other hand, KEP depletes the electron density in the binding site of functional group to C_{60} and concentrates it around the electronegative atoms of functional groups. Therefore, both KEP and OR are effective factors in promoting the binding tendency of C_{60} derivatives to enzyme. However, the OR is more important because of producing greater values of displaced charge.

Binding sites of functional group to the C_{60} almost affects the values of deformation density and displaced charge. Connection of functional group to the 5,6-junction in amino acid-type derivatives of C_{60} produces more deformation density than 6,6-junction. It is expected that C_{60} derivatives in which the functional group is attached to a 5,6-junction have more potency of bonding to enzyme.

Considering all six considered compounds and the corresponding deformation densities indicate that the suggested compound 5, has the highest OR, KEP, and total reorganized electron density. Among the C_{60} -based agents, it can be a good candidate to supply an electrostatic interaction.

The results also show that calculations at different levels of density functional theory which include dispersion interactions into electron density, fairly agrees with those without dispersion interactions. Also, the use of polarization basis functions does not affect significantly on the space responsible for charge reorganization and their corresponding displaced charge values.

Acknowledgments The authors would like to acknowledge the reviewers for their valuable comments and generous suggestions to improve the manuscript.

References

- Steinmetz NF, Hong V, Spoerke ED, Lu P, Breitenkamp K, Finn MG, Manchester M (2009) Buckyballs meet viral nanoparticles: candidates for biomedicine. *J Am Chem Soc* 131:17093–17095
- Bakry R, Vallant RM, Najam-ul-Haq M, Rainer M, Szabo Z, Huck CW, Bonn GK (2007) Medicinal applications of fullerenes. *Int J Nanomedicine* 2(4):639–649
- Nakamura E, Tokuyama S, Yamago S, Shiraki T, Sugiura Y (1996) Biological activity of water-soluble fullerenes. structural dependence of DNA cleavage, cytotoxicity, and enzyme inhibitory activities including HIV-protease inhibition. *Bull Chem Soc Jpn* 69:2143–2151
- Iwata N, Mukai T, Yamakoshi YN, Hara S, Yanase T, Shoji M, Endo T, Miyata N (1998) Effects of C₆₀, a fullerene, on the activities of glutathione s-transferase and glutathione-related enzymes in rodent and human livers. *Fuller Sci Technol* 6:213–226
- Mashino T, Okuda K, Hirota T, Hirobe M, Nagano T, Mochizuki M (2001) Inhibitory effect of fullerene derivatives on glutathione reductase. *Fuller Sci Technol* 9:191–196
- Wolff DJ, Mialkowski K, Richardson CF, Wilson SR (2001) C₆₀ - fullerene monomalonate adducts selectively inactivate neuronal nitric oxide synthase by uncoupling the formation of reactive oxygen intermediate from nitric oxide production. *Biochemistry* 40:37–45
- Ruoff RS, Tse DS, Malhotra R, Lorents DC (1993) Solubility of fullerene in a variety of solvents. *J Phys Chem* 97:3379–3383
- Brettreich M, Hirsch A (1998) A highly water-soluble dendro[60]fullerene. *Tetrahedron Lett* 39:2731–2734
- Durdagi S, Supuran CT, Strom TA, Doostdar N, Kumar MK, Barron AR, Mavromoustakos T, Papadopoulos MG (2009) In silico drug screening approach for the design of magic bullets: a successful example with anti-HIV fullerene derivatized amino acids. *J Chem Inf Model* 49:1139–1143
- Sijbesma R, Srdanov G, Wudl F, Castoro JA, Wilkins C, Friedman SH, DeCamp DL, Kenyon GL (1993) Synthesis of a fullerene derivative for the inhibition of HIV enzymes. *J Am Chem Soc* 115:6510–6512
- Friedman SH, DeCamp DL, Sijbesma R, Srdanov G, Wudl F, Kenyon GL (1993) Inhibition of the HIV-1 protease by fullerene derivatives: model building studies and experimental verification. *J Am Chem Soc* 115:6506–6509
- Calvaresi M, Zerbetto F (2010) Baiting proteins with C₆₀. *ACS Nano* 4:2283–2299
- Friedman SH, Ganapathi PS, Rubin Y, Kenyon GL (1998) Optimizing the binding of fullerene inhibitors of the HIV-1 protease through predicted increases in hydrophobic desolvation. *J Med Chem* 41:2424–2429
- Bosi S, Da Ros T, Spalluto G, Balzarini J, Prato M (2003) Synthesis and anti-HIV properties of new water-soluble bis-functionalized [60] fullerene derivatives. *Bioorg Med Chem Lett* 13:4437–4440
- Bosi S, Ros TD, Spalluto G, Prato M (2003) Fullerene derivatives: an attractive tool for biological applications. *Eur J Med Chem* 38:913–923
- Mashino T, Shimotohno K, Ikegami N, Nishikawa D, Okuda K, Takahashi K, Nakamura S, Mochizuki M (2005) Human immunodeficiency virus-reverse transcriptase inhibition and hepatitis C virus RNA-dependent RNA polymerase inhibition activities of fullerene derivatives. *Bioorg Med Chem Lett* 15:1107–1109
- Gu J, Wang J, Leszczynski J (2004) H-bonding patterns in the platinated guanine-cytosine base pair and guanine-cytosine-guanine-cytosine base tetrad: an electron density deformation analysis and AIM study. *J Am Chem Soc* 126:12651–12660
- Guerra CF, Handgraaf JW, Baerends EJ, Bickelhaupt FM (2004) Voronoi deformation density (VDD) charges: assessment of the Mulliken, Bader, Hirshfeld, Weinhold, and VDD methods for charge analysis. *J Comput Chem* 25:189–210
- Gohda T, Ichikawa M, Gustafsson T, Olovsson I (2000) X-ray study of deformation density and spontaneous polarization in ferroelectric NaNO₂. *Acta Cryst B* 56:11–16
- Johnson ER, Keinan S, Sanchez PM, Contreras-Garcia J, Cohen AJ, Yang W (2010) Revealing noncovalent interactions. *J Am Chem Soc* 132(18):6498–6506
- Contreras-Garcia J, Johnson ER, Keinan S, Chaudret R, Piquemal JP, Beratan DN, Yang W (2011) NCIPLOT: a program for plotting noncovalent interaction regions. *J Chem Theory Comput* 7:625–632
- Gillet N, Chaudret R, Contreras-Garcia J, Yang W, Silvi B, Piquemal JP (2012) Coupling quantum interpretative techniques: another look at chemical mechanisms in organic reactions. *J Chem Theory Comput* 8:3993–3997
- Fakhraee S, Azami SM (2009) Orbital representation of kinetic energy pressure. *J Chem Phys* 130:084113
- Pakiari AH, Fakhraee S, Azami SM (2008) Decomposition of deformation density into orbital components. *Int J Quantum Chem* 108:415–422
- Weisskopf VF (1975) Of atoms, mountains, and stars: a study in qualitative physics. *Science* 187:605–612
- Weinhold F, Landis CR (2003) Valency and bonding: a natural bond orbital donor-acceptor perspective. Cambridge University Press, Cambridge, p 37
- Ermakov AI, Merkulov AE, Svechnikova AA, Belousov VV (2004) Basis set orbital relaxation in atomic and molecular hydrogen systems. *J Struct Chem* 45:923–928
- Stone AJ (1996) The theory of intermolecular forces. Oxford University Press, Oxford
- Frisch MJ, Trucks GW, Schlegel HB, Scuseria GE, Robb MA, Cheeseman JR, Montgomery JA, Vreven T, Kudin KN, et al. (2003) Gaussian 03, revision B.03. Gaussian Inc, Pittsburgh, PA
- Gaussian, Inc (2000–2008) GaussView 5.0. Gaussian, Inc. copyright (c) Semichem, Inc., www.gaussian.com
- Grimme S (2011) Density functional theory with london dispersion corrections. *WIREs Comput Mol Sci* 1:211–228
- Zhao Y, Truhlar DG (2008) The M06 suite of density functionals for main group thermochemistry, thermochemical kinetics, noncovalent interactions, excited states, and transition elements: two new functionals and systematic testing of four M06-class functionals and 12 other functionals. *Theor Chem Account* 120:215–241
- Schaefer A, Horn H, Ahlrichs R (1992) Fully optimized contracted Gaussian basis sets for atoms Li to Kr. *J Chem Phys* 97:2571–2577
- Schaefer A, Huber C, Ahlrichs R (1994) Fully optimized contracted Gaussian basis sets of triple zeta valence quality for atoms Li to Kr. *J Chem Phys* 100:5829–5835
- Frisch MJ, Trucks GW, Schlegel HB, Scuseria GE, Robb MA, Cheeseman JR, Scalmani G, Barone V, Mennucci B, et al. (2009) Gaussian 09, revision A.02. Gaussian Inc, Pittsburgh, PA
- Durdagi S, Mavromoustakos T, Chronakis N, Papadopoulos MG (2008) Computational design of novel fullerene analogues as potential HIV-1PR inhibitors: analysis of the binding interactions between fullerene inhibitors and HIV-1 PR residues using 3DQSAR, molecular docking and molecular dynamics simulations. *Bioorg Med Chem* 16:9957–9974
- Lee VS, Nimmanpipug P, Aruksakunwong O, Promsri S, Sompompisut P, Hannongbua S (2007) Structural analysis of lead fullerene-based inhibitor bound to human immunodeficiency virus type 1 protease in solution from molecular dynamics simulations. *J Mol Graph Model* 26:558–570
- Grimme S (2006) Semiempirical GGA-type density functional constructed with a long-range dispersion correction. *J Comput Chem* 27:1787–1799
- Grimme S (2006) Semiempirical hybrid density functional with perturbative second-order correlation. *J Chem Phys* 124:034108